Miniature Untethered EEG Recorder Improves Advanced Neuroscience Methodologies

Chris Bailey, Jim Austin, Bettina Platt, Anthony Moulds, and Barry Crouch

Abstract—Rodent electroencephalography (EEG) in preclinical research is frequently conducted in behaving animals. However, the difficulty inherent in identifying EEG epochs associated with a particular behavior or cue is a significant obstacle to more efficient analysis. In this paper we highlight a new solution, using infrared event stamping to accurately synchronize EEG, recorded from superficial sites above the hippocampus and prefrontal cortex, with video motion tracking data in a transgenic Alzheimer's disease (AD) mouse model. Epochs capturing specific behaviors were automatically identified and extracted prior to further analysis. This was achieved by the novel design of a ultra-miniature wearable EEG recorder, the NAT-1 device, and its in-situ IR recording module. The device is described in detail, and its contribution to enabling new neuroscience is demonstrated.

Index Terms—Experimental neuroscience, EEG recording, low-power sensors.

I. INTRODUCTION

THE major healthcare challenges facing developed countries result from diseases of middle and old age. As such, modern medical science relies upon modelling human disease processes in genetically modified animals in order to understand disease pathology and develop novel therapeutics. Mice are by far the most commonly used species accounting for 74% of experimental procedures conducted on genetically modified organisms. Within the field of neuro-degenerative research, monitoring neural activity via electroencephalography (EEG) potentials in rodents provides a valuable insight into loss of brain function in disease-states and mechanisms of recovery with drug treatment. Wireless, miniature, head-mounted EEG devices are considered a substantial innovation in animal welfare over previous technologies. However, there is also both an ethical and legal imperative to mitigate the welfare impact of EEG recording on test subjects. Considering the small body mass of mice (20-30g), improved welfare can be best accomplished through reduction of device weight. Meeting this demand not only preserves the ability to undertake such research, but as will be highlighted in this paper, it can enable new methodologies and support new discoveries in neuroscience through innovation at the level of sensors and ultra-miniature systems. In this paper, the authors describe the design, implementation and capabilities of an ultra-miniature sensor, the NAT, and its recent validation through use in innovative neuroscience applications, including new neuroscience methodologies enabled by the novel capabilities of the device. In particular, it is observed that combining

E-mail (University of York): chrisb@cs.york.ac.uk
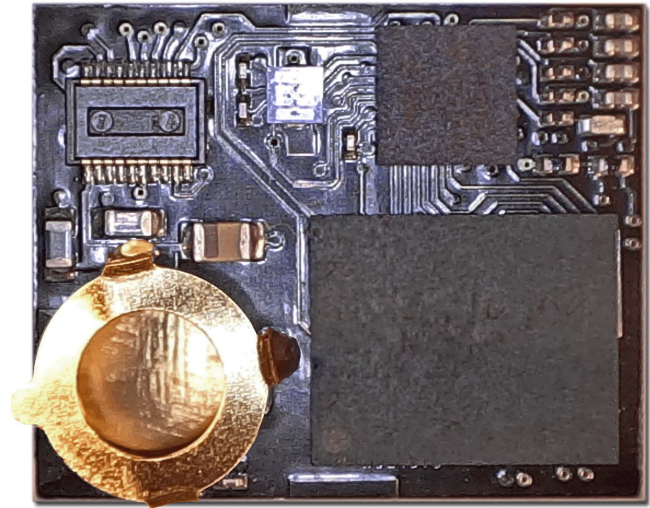E-mail (University of Aberdeen): b.platt@abdn.ac.uk

Fig. 1. NAT-1 (Neural Activity Tracker) close-up picture of top-view of device. Visible dimensions are 18x22mm. Top-Left shows expansion socket, bottom-left shows circular gold-plated custom battery-clip.

infrared (IR) event-stamping (a notable feature of the NAT-1 device), with video motion tracking, enables rapid, automated and sensitive EEG phenotyping of Alzheimers Disease (AD) mouse models [1]. This approach has also proven valuable in achieving the precise synchrony between behavioral and electrophysiological data records required to make use of novel time resolved quantitative EEG analyses.

In this paper, the first detailed technical report of the NAT device deployed in a clinical neuroscience context is introduced. Technical details of its important features and engineering rationale are presented, followed by an overview of exemplary neuroscience research studies conducted with the NAT-1 device. It will be demonstrated that the NAT-1 device, with its IR capability, has enabled a step-change in small animal EEG methodology, and as such, new neuroscience methodologies have become viable, with exciting possibilities for future advances.

Experiments described in this paper involve animal models of brain disorders and are part of larger ongoing medical research projects at the University of Aberdeen. Previously established surgical procedures are described in detail elsewhere [1], [2]. Ethical considerations of this work are considered in section V.

II. Brief Review Of The Field

The use of EEG recording in rodents, and particularly in mice, for neuroscience, is well established, with diverse methodologies [3]. Methods often combine both behavioral and physiological monitoring of subjects under carefully controlled test conditions, allowing the validation of neuroscience hypotheses and/or evaluation of pharmacological effects for therapeutic discovery [4]–[7]. Experimental set-ups often entail video observation of freely behaving subjects as they explore specialized habitats such as the Y-maze [8], [9], T-maze [10], or an open field [11], [12].

Behavior is then monitored and analysed, using advanced video motion tracking software platforms such as AnyMaze™ [13], [14], Panlab Smart™ [15], and also open community originated platforms such as OpenVEEG [16].

Such methods are often combined with simultaneous EEG recordings. This can be based on a tethered system, whereupon implanted electrodes are physically wired to signal amplification and recording hardware. This approach allows high frequency sampling, and large numbers of channels can be used in real-time data collection [3], [17], [18]. However, such systems impose welfare disadvantages, particularly the restriction of movement, and interference with normal behavior. They also impose constraints on experimental design; for example, animals cannot enter an enclosed space or a running wheel while connected to a tether. Consequently, the interest in untethered systems has been growing in recent years, with two main types of system currently available. Real-time wireless data recorders utilize a (often unreliable) radio link from a rodent mounted device to a base-station receiver, and transfers data as they are captured [19]. Some systems, such as DSI TA10ETA-F20™ are wholly implantable, though this class of device can be limited in terms of channels and sample rates achievable [20]. The alternative method is to record data onboard a removable wireless device for a period of time, then perform offline data access at the end of the experiment [1], [2], [21]–[25]. The use of onboard recorders provides an advantage in terms of reducing power consumption (as data transmission is a power hungry operation), and typically allows a reduction in circuit size, eliminating analog RF circuitry. Consequently, uninterrupted and continuous recording times may potentially extend into hours or days, even at relatively high sample rates of the order of 1KSa/s, and recording of 4 to 8 information channels. This latter scenario is the domain where the device presented in this paper is to be found. It should be noted that over-constraining of sample rates causes a number of problems, which can only be avoided with careful attention to bandwidth limiting of input signals [26], yet even in this case, the temporal resolution of EEG event correlation suffers when overly low sample rates are used.

III. Development context

The NAT-1 (Neural Activity Tracker) is a highly miniaturized wireless electronic recording system, developed by the University of York, University of Aberdeen, and Cybula Ltd., in an industry- academic partnership, with specific applications in rodent-based neuroscience. However, the compactness,

lightweight properties, and long recording times of the device, without any base-station requirement, also make it useful in a range of non-invasive applications [24], [25].

The team at the University of York[1] specialize in sensor platforms, miniature electronic systems design and manufacture, and complex data analytics. The team at the University of Aberdeen[2] have a longstanding international reputation for neuroscience in the context of rodent EEG monitoring for both neural studies, and pharmaceutical evaluations via neural impact studies. Cybula Ltd. is a privately owned company engaged in advanced data analytics systems delivery and academic-industry technology transfer.

The NAT-1, a view of which is shown in Figure 1, was designed specifically to support neural studies in rodents, and validated by the collaborative team at the University of Aberdeen. A broad range of experimental studies have already been undertaken with the utilization of NAT-1 devices [1], [2], and several are described in more detail, from a circuit/sensor perspective, in this paper.

A. Ethical Considerations

Preclinical and translational neuroscience research relies on modeling human disease processes in genetically modified or pharmacologically treated animals, most commonly mice or rats. Welfare considerations have become increasingly pertinent, as regardless of the species, there remains an ethical and legal imperative to utilize the least harmful experimental technique available and optimize the ultimately essential use of experimental species (3R principle: Reduce, Replace, Refine). In the realm of *in vivo* electrophysiology, wireless EEG recording systems are now considered a substantial welfare improvement over traditional tethered or implanted systems as recordings can be conducted in the same specimen over many months or even years. Weight-wise, 10% of body mass is generally considered the acceptable maximum for head mounted devices in rodents. Therefore, while the majority of *in vivo* medical research utilizes mouse models, their small body mass (20-30g) relative to that of rats (400-800g) creates a significant design challenge for wireless EEG systems, especially where extended recording periods are desired (and thus larger battery capacity).

IV. Technical Description

The NAT-1 system module, as detailed in Figure 2, is designed around a combination of (a) a custom discrete analogue electronics front-end, (b) a standard low-power microcontroller, including on-board Analogue-to-Digital Converter (ADC), (c) a multi-gigabit flash memory storage chip, (d) a multi-purpose daughter-board expansion socket, and (e) a custom designed gold-plated battery clip. Adding a standard A13/PR48 type zinc-air battery, allows the device to be powered up and active, and in this state, its total weight is less than 2.3 grams, its height profile at maximum extent is less than 10mm (primarily due to the battery shape and size), and its footprint dimensions are only 18mm by 22 mm.

[1]Bailey, Austin, Moulds: Advanced Computer Architectures Group, Department of Computer Science, University of York, UK

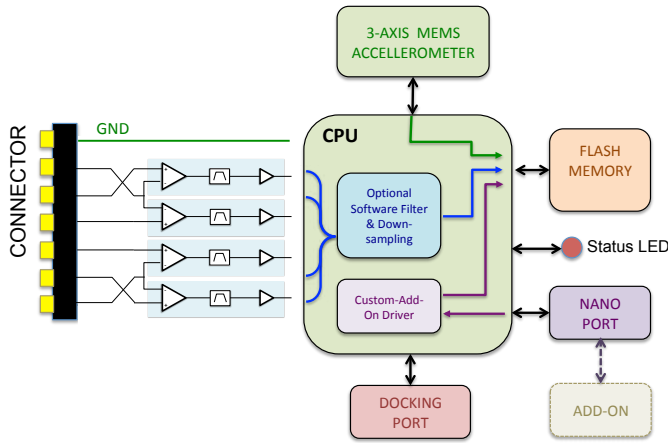[2]Platt, Riedel, Crouch: University of Aberdeen, UK

Fig. 2. NAT-1 system component diagram

Fig. 4. Underside of NAT-1 device, showing analogue electronics components and head-connection interface. In addition, gold-plated corner pads can be seen, which provide interfacing to a docking station when required.
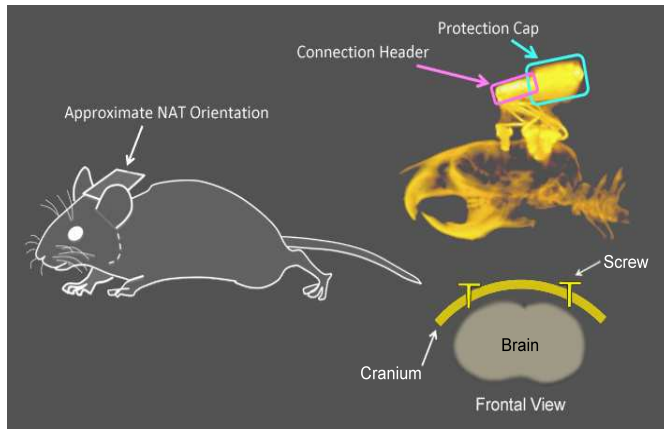

Fig. 3. Typical orientation of head-mounted device, and CT scan of header (with protection cap fitted, no NAT-1 present). Example of frontal projection shows screw positions not easily determined in CT side view.

Fig. 5. NAT-1 Electrode input model, showing (a) one of two pairs of analogue input channels, with instrumentation amplifiers, each sharing common (local) reference input, (b) band-pass filters stages, and (c) programmable amplifiers.

The NAT-1 device is designed to be head-mounted on small rodents (rats and mice in particular), and is secured via a surgically implanted electrical connector port, which in turn is held in situ by cyano-acrylate adhesive, and dental cement. This provides intra-cranial electrodes (for example, small gold-plated screws), with external leads, and a mating connector which also locates the board and its orientation in a position relative to the rodent cranium that provides minimal external disturbance of normal subject behavior. Figure 3 shows this scenario, with a computed tomography image (side projection) of a mouse head-stage utilizing epidural screw type electrodes. Note that due to the curvature of the skull, laterally placed electrodes appear in a 2D image to be implanted far deeper than they are in reality. The frontal view aspect illustrates this principle.

The device can easily be removed when not in use, but can be worn for periods up to 5 days in one session, with recording times varying according to sample rates, as discussed later. An on-board indicator-LED provides occasional information feed-back cues for the experimenter, such as power-up confirmation, start of recording alert, error status and recording end conditions.

Fig. 6. Relationship between brain and electrode inputs, showing intracranial EEG electrodes with common ground reference. Note: PFC - Pre-frontal Cortex, HC - Hippocampus. Electronic components: (a) instrumentation amplifiers, (b) unity gain buffer, providing conditioned ground reference.

A. Analogue Front-End Design

The analogue front-end stage is comprised of discrete analogue components located on the underside of the NAT-1 device, as noted in Figure 4. Provisions are made for up to four simultaneous EEG electrode measurements arranged in two pairs; each input pair sharing a separate reference electrode, as shown in Figures 5 and 6. A comprehensive review of electrode placement considerations is given in [3], and further discussion is provided in later sections of this paper. A gr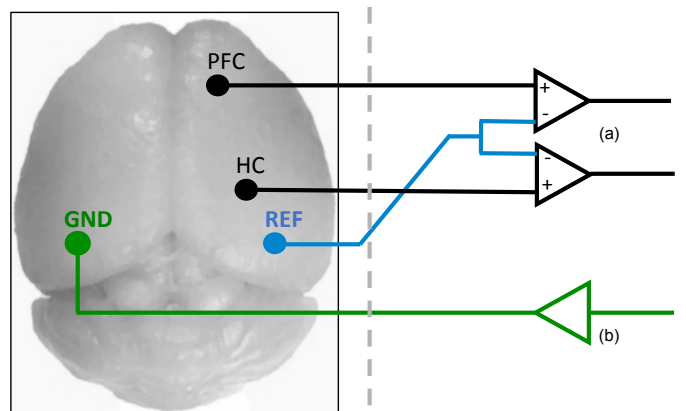ound reference output is provided in order to set the ground potential for all input signals. High-impedance low-noise instrumentation amplifiers (IAs) are used in the NAT-1 device to directly amplify the voltage difference between the analogue input signal and its associated reference input.

An important aspect of the design, and particularly for the NAT-1, is the sampling regimen. This includes the important consideration of anti-aliasing, well explained in terms of EEG signal acquisition [26]. Additional components enable the input channels to perform band-pass filtering on the input signal. A second-stage amplifier adds further signal gain and low-pass filter for improved high-frequency roll-off. The quarter-power bandwidth for each band-pass-filtered analogue channel is fixed between 0.2 Hz and 500 Hz, as shown in Figure 7.

Due to the variety of voltage magnitudes that can be obtained in EEG and local field-potential measurements, the signal gain of the combined front-end and on-chip microcontroller A/D Converter (ADC) can be parametrically configured via software control. This results in a selectable peak voltage input range from three possible choices; 1, 2 or $4\,\text{mV}$. Each channels range can be configured individually. The ADC input signal resolution is $0.5\,\mu\text{V}$, $1.0\,\mu\text{V}$ and $2.0\,\mu\text{V}$, for the corresponding $1\,\text{mV}$, $2\,\text{mV}$ and $4\,\text{mV}$ amplitude ranges, respectively.

The majority of spectral power in an EEG signal is below 50Hz (corresponding to Delta-Gamma EEG bands) and typically falls away at 3dB/octave (1/f response) [27]. The channel band-pass filter described above offers good group delay response for maintaining acceptable amplitude envelope fidelity, in the range suited to EEG data.

B. Data Conversion and On-board Signal Processing

The NAT-1 device uses an ATXMEGA32™ microprocessor, with on-chip ADC data converter. Four analogue EEG field potentials (or indeed any suitable analogue signal source) can be digitized by the ADC in sweep mode. The microcontroller's on-chip 12-bit sigma-delta ADC digitizes the conditioned analogue signal in 11-bit signed integer format. With the front-end bandwidth of 500Hz and anti-aliasing filter of 60dB/decade shown in the frequency plot of Figure 7, the full bandwidth dynamic range (DR) at a sample frequency $\mathbf{f_s}$ of 6kHz is 50dB. However, for the primary application of EEG signal measurements where the source bandwidth is sub-50Hz, $\mathbf{f_s}$ can be reduced to 2kHz, while still offering a useful dynamic-range of 52dB. Lower sample rates can be set at the expense of reduced dynamic-range, or when the power-spectral-density (PSD) in the signal falls off more sharply. Lowering the sample rate is desirable when long-duration recordings are required,
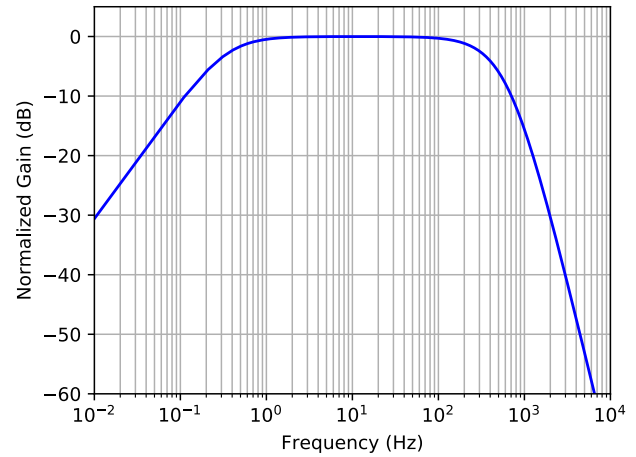

Fig. 7. Characteristics of NAT-1 input-channel frequency response, showing gain (normalized) bandwidth of front-end analogue channels, with quarter-power bandwidth set between 0.2 Hz to 500 Hz.

TABLE I
RECORD TIME, AND POWER CONSUMPTION, VS. SAMPLE RATE

Fs (Hz)	DR[1] (dB)	DR[2] (dB)	Power[4] (mW)	Rec. Time[5] (Hrs)	Battery Life[6] (Total Hrs)
2000	52	68 [3]	6.4	9 / 18	50
1000	34	68	5.1	18 / 36	64
500	28	56	4.4	35 / 70	76
250	22	44	4.0	70 / 83[5]	83

EEG with 1/f PSD, [2] EEG with 1/f2 PSD, [3] Limited by ADC,
[4] Continuous operating power. [5] Based on 4Gbit, and 8Gbit flash-memory capacities. At lower sample rates, recording time becomes battery limited.
[6] Assuming repeated recordings, or suitably sized flash memory, using Duracell DA13 Zn-Air battery.

since power consumption is proportional to $\mathbf{f_s}$. Typical operational record times versus sample-rate comparisons are given in Table I, alongside record times, power consumption, and battery life, where dynamic range (DR) is applicable to EEG sources only. Interestingly, flash capacity limits record time at high sample rates. However, at the very lowest sample rates, it is battery capacity that starts to limit record time. For example at 250 Sa/s, record time will be no more than 83Hrs, due to battery life, even though an 8Gb flash version of NAT (NAT-1-8G) has a theoretical 140hr recording capacity at that sample rate. Achieving a balance between exacting weight constraints and long record times at low sample rates, is a key reason for choosing the zinc-air power cell.

One important observation is that when the signal source bandwidth is limited, but subject to noise or spurious higher frequencies, it can be wasteful storing and downloading samples taken at the default sample rate. Firmware in the on-board microcontroller includes the option to perform software filtering using a simple block averaging operation, on real-time sample data, and then only stores the resulting filtered samples. This is a form of down-sampling as defined by equation 1.

$$BA[j] = \sum_{i=0}^{N-1} \frac{s[j-i]}{N} \qquad (1)$$

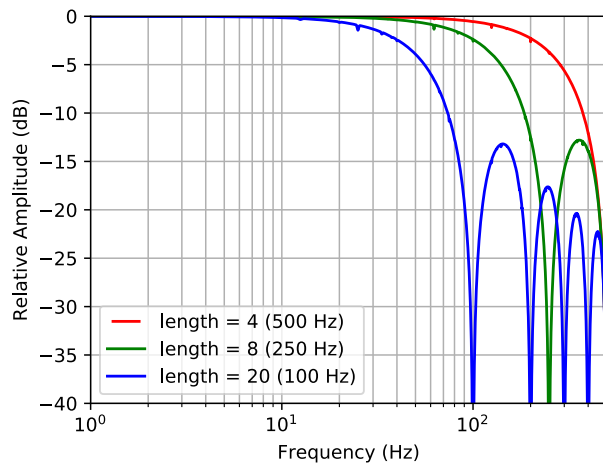*Where N = block length, i = sample, and BA[j] = block-averaged sample.*

Fig. 8. Effective frequency response of Block Average filter for different values of Block Length (N) with f_s=2kHz.
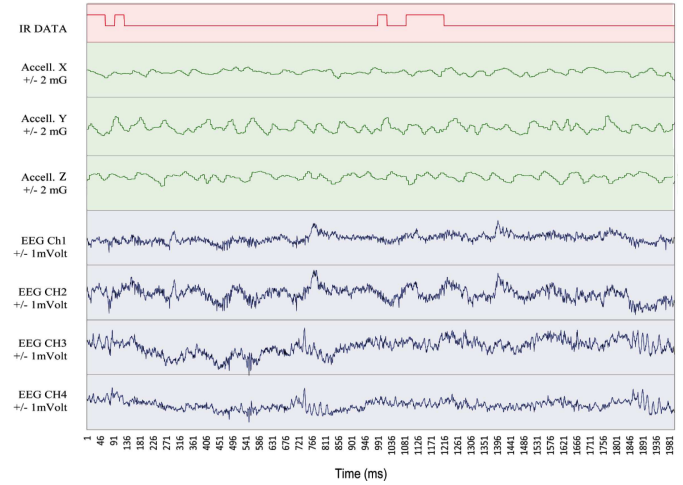

Fig. 9. NAT-1 data capture results, showing infrared data recording (red), accelerometer (green, 3-axis X/Y/Z), and 4-channel EEG programmable field-potential sensing (blue).

Although this moving-average filter is computationally low-cost, its frequency response, and high-frequency roll-off, is not hugely effective - it is a compromise. In general the frequency response of this approach can be represented by equation 2.

$$H[f] = \frac{sin(\pi f N)}{N sin(\pi f)} \qquad (2)$$

Where H[0]=1, and f = 0 to 0.5.

Then, the signal attenuation at a given a frequency of interest f_i, is found for H[f] when f satisfies equation 3.

$$f = \frac{f_i}{f_s} \qquad (3)$$

For example, at a 2kSa/sec master sampling rate, and N=5, the averaging filter and down-sampling will result in a new effective sampling rate of 400Sa/sec. A signal component at f_i = 200Hz, whereby f = 0.1, will be attenuated to around 65% of full strength. Aliasing is therefore reduced but not completed eliminated in this mode. An example of such a frequency response is given in Figure 8.

The BA algorithm acts as a simple smoothing filter on the sampled data and requires very few lines of code to implement. More sophisticated filtering techniques may be used, but these are best achieved by recording data at the full sample rate and then down-sampling after download of the data file to a desktop computer or similar computing platform, otherwise the trade-off between processing and recording power starts to become undesirable, and recording times would be reduced unnecessarily.

Since the attenuation profile of the software filters is relatively shallow at the start of roll-off, this behavior should be considered carefully where relative power of individual frequency components is important for analysis.

Simultaneous to the acquisition of 4-Channel EEG, a 3-axis Micro-Electro-Mechanical-System (MEMS) accelerometer with selectable 2G/8G range, and 8-bit digital output, is also sampled. This device, consuming only 18µW when active,

permits kinetic 3D motions to be synchronously recorded alongside the EEG signals and external IR time-stamps, and then be correlated to video footage. The NAT-1 device can also be used purely in accelerometer mode, with extended battery lifespans, and then acts as a very small and capable wearable motion sensor [24], [25].

The accelerometer is mounted so that when worn by an animal (e.g. mouse or rat) its X-axis is aligned along the body of the animal (sagittal plane - tail to head), and its Y-axis then assumes the transverse plane of the animal. All three axis are recorded by the NAT-1 together with the EEG samples.

The accelerometer's motion bandwidth is limited to 80Hz by the characteristics of the MEMS device, and reduced to 20Hz for system sample rates below 400Sa/sec. Meanwhile, two accelerometer ranges are selectable; +/- 2G and +/- 8G, offering 18mG and 56mG sensitivity respectively. Figure 9 shows an example of the full data capture capabilities of the NAT-1 device, including the infrared data-stream recording facility (via the IRDB daughter-board described later).

In this figure one can see the various data types that the NAT-1 can simultaneously capture. The topmost trace 'IR DATA' (colorised red) shows the continuous data recording from the IR sensor, including some binary data packets captured during recording. The traces immediately below, colorised green, and labelled 'Accell. X', 'Accell. Y' and 'Accell. Z', represent the X,Y and Z accelerometer channels. Finally, the bottom four traces (colorised in blue) represent four analog input channels, in this case recording EEG potentials with a +/-1mV range, but also able to support a wide range of other compatible recording sources across many domains.

C. FlashMemory

The on-board flash memory presents some interesting design challenges for such a small device. The NAT-1 utilizes a 4Gbit flash memory chip; an 8Gbit memory is available as an option. Whilst the average power consumption of flash memory in the NAT-1 device is low, its power demand

is transient, with most of the power consumed during the page program phase, typically 18mW lasting 500μs. Page programming occurs periodically as the write page fills up with sample data; this interval is determined by the chosen sample rate. The interval is significantly longer than the page program transient power event, enabling the power to be delivered from local decoupling capacitors, giving enough time for the power management unit sourced from the Zinc-Air battery to recover and prevent system voltage droop. As a result, flash-memory peak-power demand is met at all operational sample rates without degrading main processor and auxiliary component power availability.

Flash integrity is an important further consideration, common to most non-volatile memory applications. The NAT-1 microcontroller's firmware implements a bad-block table in flash memory. Any bad blocks detected during erasure are marked and ignored for recording purposes. The table is updated by host software during the download process. To protect the flash memory from data corruption and block damage due to undesirable power cycling, the firmware continuously monitors the health of the battery. The NAT-1 device shuts-down in a controlled fashion when the battery is weak, and prevents further operation until this status condition is cleared during data download.

D. Nanoport daughter-board Connector

As noted earlier, a miniature multi-purpose expansion socket is provided, the 'nanoport', which allows for custom daughter-board augmentation of the sensor capabilities. This feature has proved to be very valuable, since it has allowed specialized capabilities to be added to the validated core system and thus to rapidly enable new neuroscience methodologies, as will be described later. The connector provides power and SPI (Serial Peripheral Interface) data connectivity, theoretically allowing a wide range of auxiliary daughter-boards to be designed around SPI-capable sensor devices, expansion memories, transmitters and/or receivers, or even conceivably a co-processor module. In particular, the team have developed an infrared detector-board (IRDB), which has been utilized effectively for time-stamping and event registration device in various neuroscience scenarios, such as maze testing. This is expanded upon in a later section of this paper.

E. Custom Battery Clip and Power Management

An important requirement of the NAT-1 recording device is the reliability of the battery attachment. No off-the-shelf lightweight solution was available, resulting in the requirement to develop and validate a bespoke design.

The bespoke battery holder, shown in Figure 10, is designed to house a single zinc-air battery of type A13/PR48. This battery, which is inexpensive, and widely available for use in hearing-aids, provides a very high power density, which is ideal given the exacting constraints on weight and size of the NAT-1 device. The contrast between the Zinc-Air A13 cell and other small battery cells, shown in Table II, highlights the high power capacity, and vastly superior power density of this cell
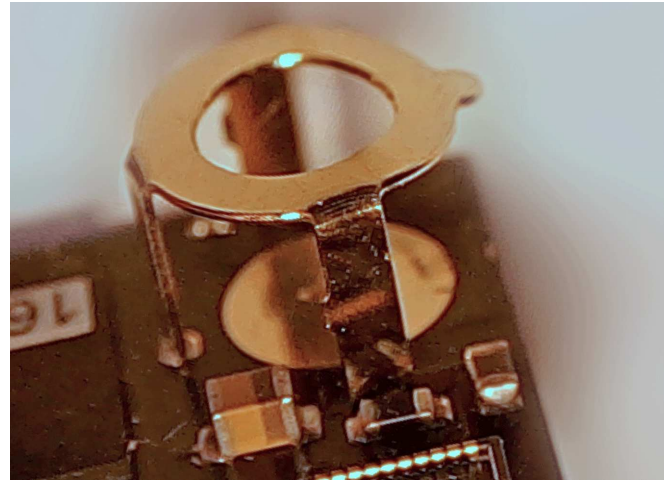

Fig. 10. Specialized custom battery-retention clip.

type, particularly when contrasted with alternatives recently surveyed elsewhere [28].

This is achieved because the cell actually performs a chemical reaction with air entering the cell via carefully engineered pores in the battery case, resulting in continuous low level power availability until expiration. Although a rechargeable device would be highly desirable, at present there is no solution that can match the performance of the A13 cell and work reliably while fitted onto a moving animal.

The NAT-1 battery holder does not simply provide an electrical connection for power. One of the challenges of rodent monitoring is that their behavior can often compromise the battery connectivity. Sudden movement and vibrations can momentarily disconnect the power source, leading to signal glitches, brown-outs, or processor program errors. Worse still, batteries can be dislodged completely, leading to wasted experimental effort and time. In order to avoid this, a bespoke battery-clip design was devised.

The battery holder is manufactured from a beryllium-copper alloy, and is gold-plated to offer high electrical conductivity and low corrosion properties. The three legs shown in the image provide rigid stability to the holder frame while the cap is sprung at its leading edge to hold-back the battery once inserted. The entire pre-formed holder is age-hardened at 350° centigrade before assembly to induce the desired spring effect.

This design has proven to be highly reliable. In hundreds of real rodent test cases, no occurrences of battery displacement have been observed to date, and no detection of intermittent power glitches have been reported.

TABLE II
BATTERY TYPES AND POWER CHARACTERISTICS

A13/PR48	Zinc Air[1]	280 mA h	333 mAh/g
CR2032/ECR2032	Coin Cell[2]	230 mA h	77 mAh/g
LR44/A76/V13GA	Button Cell[3]	105 mA h	60 mAh/g
LR43/AG12	Button Cell[4]	55 mA h	26.1 mAh/g
PR70/AC10	Button Cell[5]	70 mA h	233 mAh/g

[1]0.84g,Dia.7.8mm,H5.4mm,1.4v, [2]3.0g,Dia.20mm,H.3.2mm,3.0v, [3]1.75g,Dia.11.4mm,H5.6mm,1.5v, [4]2.1g,Dia.11.6mm,H4.2mm,1.5v [28], [5]0.3g,Dia.5.7mm,H3.5mm,1.5v [28]
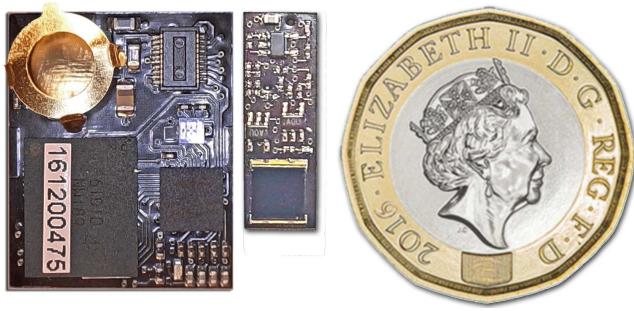
Fig. 11. IRDB Board (middle), compared to NAT-1 device (left), with UK one-Pound coin for scale (almost same size as a one-Euro coin), all sizes approximately to scale.

Fig. 12. NAT-1-IRDB Spectral sensitivity characteristics, showing (a) optical sensitivity and (b) sensitivity to angular source placement.

A critical design requirement for the NAT-1 device is power efficiency. A single Zinc-Air battery powers the entire recording device. The nominal 1.2V DC voltage from the battery is up-scaled by a step-up synchronous DC-DC converter to power the NAT-1. The converter operates at high efficiency, limiting conversion losses to just 17%. The frequency of its switching oscillator is fixed at 2MHz, ensuring a useful margin exists beyond the NAT-1 device's analogue front-end bandwidth. The analogue and digital components are powered from separate supply voltages and aggressively decoupled. The analogue supply has additional filtering for improved noise performance. On power-up, when the battery is first inserted into its holder, the DC-DC converter is held-off while the input bulk capacitor is fully charged. This capacitor is placed in parallel with the battery to rapidly supply fast transient load currents during normal operation; this is essential since the battery's demand-response time is relatively slow.

F. Daughter-board options and the NAT-1 IRDB

A versatile feature of the NAT-1 device is the miniature expansion socket. This permits additional electronics payloads to be fitted to the NAT. Of course, this comes at the cost of additional weight and power utilization. However some expansion boards can be extremely small, and consume minimal extra power. An example of this scenario is the IRDB infrared detector board, also developed by the authors, and with particular value in scenarios involving the need to time-stamp events during an experimental process, and/or for designating start/end points in individual test runs or test phases. Data processing scripts can then be used, for instance, to automatically categorize or segment data into particular subsets, events, or operational cases.

The NAT-1-IRDB daughter board, as shown in Figure 11, is extremely small (17.6mm x 5.8mm x 1.7mm) and lightweight (0.1 grams). These highly constrained physical attributes mean that, when fitted, the IRDB board does not add to the overall maximum height profile of the NAT-1 device, since the battery is still the feature with the greatest height extent for the device.

The IRDB board detects infrared impulses, with peak sensitivity at 940nm wavelength, and a wide acceptance angle, as illustrated in Figure 12, where Figure 12(a) shows wavelength sensitivity, and Figure 12(b) shows sensitivity as a function of angular source position, with respect to the sensor.
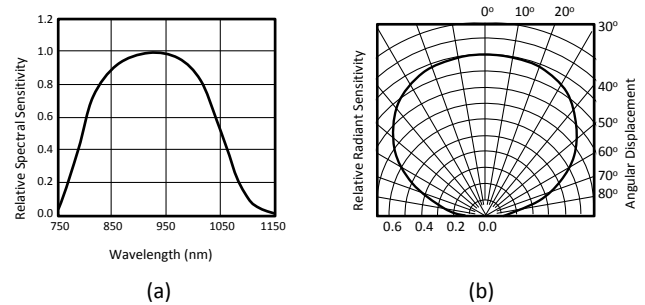
This is a spectral range that is invisible to rodents, and humans, and therefore cannot interfere with normal behaviors or neural activity. The infrared intensity is recorded on a continuous basis, with a recording rate in step with the main EEG sampling rate of the system. As a result of this design, any infrared signal may be used to provide time-synchronised event labelling cues within data. When combined with systems such as AnyMaze[TM], where proximity detection gates and other sensors can generate digital trigger signals, it is possible to convert trigger signals into infrared pulse-codes, and therefore use the IR-1 capability to align trigger events with high time resolution, against EEG post-event responses or pre-event activity.

When recording in pulse mode - where the IR signal is quantified as a binary 0/1 single-bit state, the device utilizes a hysteresis circuit to eliminate false signal transitions where weak signals are near the logic thresholds. In analogue mode, infrared signal intensity can be digitized to an 8-bit scale, and this could be exploited for a number of purposes to introduce new experimental features into neuroscience experimental setups.

An example of IRDB data-stream recording is shown in Figure 9, where a pulse code model is used to represent individual events. Coding is entirely open to the end-users as appropriate to their experimental setup. Typically, a pulse code based upon RS232 8-bit encoding protocol can be found to be highly convenient, since it contains start and stop bits to assist with accurate framing of encoded data bits. However, analogue data streams could also be utilized, or even a combination of both.

V. EXEMPLAR NEUROSCIENCE APPLICATIONS

The NAT-1 has been marketed and used in a number of commercial pharmaceutical settings as well as for academic neuroscience research programs. In this section, we reprise the published findings of several recent experiments conducted in mice which represent one of the most challenging mammalian species in which to conduct wireless electrophysiology. We hope here to highlight (a) the application utility of the device, and (b) capabilities for improved neuroscience research methodologies, with valuable outcomes for experimental practice.

A. Ethical Statement

All experiments described here and those published in previous reports, conducted at The University of Aberdeen, were approved by that universitys ethics board and carried out in strict accordance with the Animal (Scientific Procedures) Act 1986 and EU directive 2010/63/EU.

B. Surgeries

Surgical procedures used in studies discussed here are also described in detail in their respective publications [1], [2]. It should be noted that best practice surgical and aftercare procedures are influenced by local (institution), national (home office) and international (Felasa) guidelines. The precise procedures will therefore naturally vary between research teams.

After induction of general anaesthesia and removal of the periosteum from the apex of the skull, epidural screw electrodes (gold plated micro-screws wired to 0.6mm square cross-section pin terminals) were stereotaxically implanted into burr holes drilled at designated co-ordinates on the skull. A cyanoacrylate adhesive was then applied to the skull and dental epoxy (Simplex Rapid^{TM}, Kemdent, UK) was then poured onto the adhesive encasing electrodes, wiring and proximal end of the pin terminals. This result is a durable headstage which will withstand multiple recordings from chronically implanted electrodes over periods of up to 16 months after implantation [1], [29], [30]. Note that the NAT-1 board is removable, and only fitted to the headstage when in use. Animal drinking water was supplemented with carporofen (non-steroidal anti-inflammatory) for 24 hours before and 72 hours after surgery. A subcutaneous injection of buperinorphine and an intraperitoneal injection of saline were given immediately prior to recovery from general anesthesia. Animal weight, fluid intake, and physical condition were then assessed daily for two weeks of recuperation prior to first attachment of devices. While the studies described here used common epidural screw type electrodes, these are neither the only electrode available to the researcher nor a requirement for use of the NAT device. Indeed many teams prefer to simply use bare wire electrodes for recording of cortical EEG [31]. We refrain from making any recommendations of electrode type here as this choice is governed by the needs of the individual experiment. We wish to highlight however that the NAT device may read any electrode so long as its lead wire can be soldered, wrapped or otherwise connected to a compatible pin terminal.

C. Pharmacological studies including sleep behaviour of EEG

Episodes of Rapid Eye Movement (REM) and non-REM sleep cannot be differentiated in animals based on behavioural observation alone. This distinction can only be made via direct observation of brain activity. A common application of EEG in preclinical research is therefore quantification of sleep latency, depth and duration to screen for hypnotic or stimulant effects of novel drugs.

The suitability of the NAT device for pharmaco-EEG applications was recently demonstrated in an experiment where EEG was recorded following administration of the common sedative drug diazepam [1]. Analysis of EEG data captured by the NAT confirmed the rapid descent into Non-REM sleep following administration of diazepam. Reduced low frequency with increased high frequency activity in non-REM sleep, a characteristic effect of the drug [32], were also observed. Drug effects on Non-REM EEG functional connectivity was then compared between diazepam and ketamine, an anesthetic drug with paradoxical stimulant effects at low doses.

Notably, with the aid of the NAT-1, this work has thus revealed profound differences between the impact of diazepam and low-dose ketamine on communication between the pre-frontal cortex and hippocampal formation, potentially explaining their opposing effects on sleep latency.

D. Behavioral-EEG phenotyping of Alzheimers disease mouse models

Human EEG recordings are predominantly conducted in participants at rest. By contrast, rodent EEG is typically recorded in ambulatory subjects which presents with unique analytic challenges. Notably, movements can introduce artifacts, particularly in the Delta (0-5 Hz) range, and the amplitude of hippocampal Theta (5-9 Hz) and Gamma (20+ Hz) oscillations essential for neural communication and information processing [33] are heavily influenced by movement speed in rodents [34], [35]. Therefore, to study the physiological and pathological aspects of cognitively relevant EEG features, it is critical to first control for the effect of movement. This can be accomplished through co-registration of EEG data with measurements of the animals position in space. A recent study [2] has demonstrated the suitability of the NAT-1 IRDB module for this purpose and its application to pre-clinical dementia research. In this study, transgenic mice (PLB2$_{APP}$) expressing the human Amyloid Precursor Protein (APP), with the Swedish and London Alzheimers Disease AD risk mutations, underwent electrode implantation surgery at five months of age when disease pathology is known to be relatively subtle [36]. The mice were then subjected to a Y maze spontaneous alternation task. This paradigm was selected in order to assess the function of the hippocampus and entorhinal cortex, which are critical regions for memory and spatial navigation; and are impacted early in human AD. The maze itself is a simple structure consisting of three corridors meeting at a triangular intersection which the animal is allowed to freely explore for ten minutes. The EEG was recorded throughout the experiment using the NAT-1 while the animals location and behavior were continuously monitored by a computer running the AnyMaze (Ugo Basile, Italy) behavioral tracking software, which employs an overhead video camera. AnyMaze-triggered pulse trains from an overhead IR-LED array were registered by the IRDB module and used to create corresponding event stamps in both EEG and behavioral data records. A MatLab^{TM} (Mathworks, USA) script was then used to merge the two data sets into one file for subsequent analysis. A typical representation of the described technical set-up is given in Figure 13.

The study revealed firstly that PLB2$_{APP}$ display slowing of the EEG (loss of high and gain of low frequency power) characteristic of human AD, in the absence of any overt cognitive
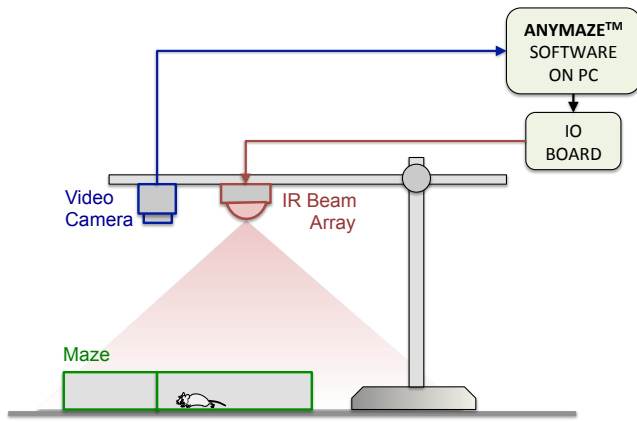
Fig. 13. Typical maze setup used at University of Aberdeen for infrared time-stamped EEG and Video observation.

differences relative to age matched wild type controls. Further analysis revealed that the positive correlation between hippocampal Gamma band (high frequency) power and movement speed, as observed in healthy mice, was absent in PLB2$_{APP}$ animals. This indicates a failure of neural systems responsible for encoding of speed in AD mice. Subsequent analyses revealed that Gamma frequency EEG activity patterns associated with movement towards the maze intersection remained intact. Cumulatively, the findings of this study indicate that under specific behavioral conditions, EEG signatures indicative of early AD pathology can be detected even in the absence of cognitive symptoms. It is hoped that studies such as this may ultimately pave the way for development of human diagnosis techniques to detect AD, at the pre-symptomatic stage, thus enabling early intervention.

VI. DETECTION OF TIME-, FREQUENCY- AND DIRECTION-RESOLVED COMMUNICATION WITHIN BRAIN NETWORKS

Neural signaling is extremely rapid, and large scale brain networks only remain stable for approximately 100ms before undergoing functional reconfiguration [37]. The recent development of time varying brain connectivity estimators enables analysis of frequency-resolved directed communication within brain networks, on time scales commensurate with those of neural signaling [38]. However, to harness the improved temporal resolution of these techniques, it is crucial that EEG samples are precisely time-locked to the event of interest. One such recent behavioral study [1] utilized the NAT-1 with IRDB enabled data synchronization, in combination with time varying renormalized partial directed coherence (TV-rPDC) analysis [38], to quantify brain network function during spatial decision making in the Y-maze.

As mice explore the approach to the Y-maze intersection, they must make a left-right choice of direction. Over multiple approaches, healthy mice display an innate tendency to choose the least recently visited of the two corridors (the correct behavior). The ratio of correct vs. incorrect choices is taken as an index of cognitive performance. However, despite the widespread use of spontaneous alternation tasks in cognitive

phenotyping, relatively little is known about the neural processes underlying the preference for correct arm choice.

One aim of the aforementioned study was therefore to analyze EEG on approach to the maze intersection using TV-rPDC in order to establish; 1) whether correct and incorrect arm choices are associated with distinct patterns of directed communication between the prefrontal cortex and hippocampus; 2) The temporal order of these patterns; and 3) The location in the maze where they occur. Using the same experimental setup as described previously, the NAT-1 and IRDB module were used to acquire samples of EEG, whilst capturing motions through a Y-maze intersection which were precisely matched for speed and location over time. Subsequent analysis broadly matched previous observation of elevated prefrontal-hippocampal synchrony occurring at maze intersections. However the use of TV-rPDC further revealed a temporal pattern of directed communication specifically preceding correct corridor choices. Most notable was the discovery that this pattern is initiated by communication in the Theta frequency band originating in the prefrontal cortex and targeting the hippocampus. This study therefore expanded on previous work by uncovering evidence for a driving role of the prefrontal cortex in spontaneous alternation behavior.

VII. THE ROLE OF ADVANCED DEVICE FEATURES IN ENHANCED NEUROSCIENCE OUTCOMES

Based on the experiences described in previous sections, and more generally in work undertaken at Aberdeen and associated partners, it is apparent that several key gains have been achieved by using the NAT-1 devices:-

- Lightweight untethered operation permits free motion testing in mazes and homecage,
- Simultaneous collection of EEG, accellerometry, and time-stamp IR-Data codes,
- High sample rates and long record times,
- Temporal correlation between related events.

It was also noted that, although all studies discussed here were conducted using a fixed gain setting of 2mV, the provision of individually configurable gain on each analogue channel is highly beneficial when recording local field potentials, where the potential differences between active and reference electrodes will vary by depth.

As a result of the employed IR-coded time-stamp methodology, the recognition of candidate events is greatly improved in terms of localization of relevant EEG data segments, making automation in conjunction with high quality of analysis more effective than possible previously. Increased automation, with increased robustness of data quality, means it is possible to process more tests more quickly and generate more rigorous overall measurements and conclusions.

The experience with untethered EEG recording for neuroscience research at Aberdeen has included of the order of 500 individual EEG recording instances with rats and mice. Between 40-50% of these recordings were conducted with NAT-1, and the remainder with other legacy devices, giving an excellent basis for comparison, and robust usability evaluation.

This reinforces confidence in the significant benefits of the NAT design.

VIII. PROSPECTS FOR FUTURE DEVELOPMENT

Following the landmark discovery of spatial maps and place cells [39], progressive study of hippocampal single unit activity has revealed further components of the brain's spatial navigation system, including grid cells [40], boundary vector cells [41] and speed cells [42]. Single unit recordings of the motor and parietal cortices have revealed similar cell systems encoding body position [43]. These discoveries have significantly improved our understanding of neural encoding (in health and disease) and may have substantial implications for future development of brain-computer interfaces and advanced prosthesis. The growing research interest in single-unit recordings has driven demand for high density electrode configurations and innovations such as exotic electrodes; notably, the recently reported injectable neural mesh [44]. Consequently, there is increasing demand for higher sampling rates and more input channels on data logging systems. In order to avoid a return to tethered systems, substantial innovation will be required to meet demand for increased functionality in wireless and wire-free devices, without a parallel increase in mass. The modular nature of the NAT-1 provides an interesting solution to this problem. Elements which may or may not be required for individual experiments (IR receiver, memory expansion, accelerometer, etc.) can be delegated to interchangeable daughter boards allowing more main device weight to be occupied by ubiquitous system components (ADC, main memory)

In terms of battery systems, there is also a significant challenge. Size and weight are always a concern, and with extended recording times, increased sample rates, and increased channel capacities, these constraints can be challenging. The ideal solution, of an extremely lightweight, compact and rechargeable power component, has yet to be realized at the scale required for such small devices. Nonetheless, battery technologies continue to develop, and system power budgets can be expected to be further trimmed as silicon devices continue to be refined. There is reason therefore to be optimistic about future improvements.

IX. CONCLUSIONS

There are numerous methods and approaches for neurophysiological research in small rodents, including tethered and non-tethered systems. The benefits of a non-tethered system are often difficult to achieve, due to weight and size restrictions, coupled with device re-usability and versatility. Nonetheless they can offer significant advantages. This paper has provided a detailed engineering description of NAT, the Neural Activity Tracker, a device for rodent-focused neuroscience research. This device has been found to be highly versatile, a valuable enabler for improved sophistication in several reported leading-edge neuroscience studies, and has contributed to better understanding of neural processes.

As discussed in Section VII, a number of notable observations from use of the device in the reported context are made. It can be concluded that there are significant benefits from having a miniature recording device with customisable daughterboard - allowing new features such as IR-sensing to be added, and thus augmenting the capabilities of neurological studies to address specific needs. The use of zinc-air batteries is also a relatively uncommon choice in similar designs, but offers a valuable power capacity advantage, and this is again important for add-on boards. The IR-Board consumes less than 110µW worst-case power, but other modules may require more, and the chosen battery can cope with the power requirements well, even over long recording sessions, but without creating weight concerns. Finally, the ability to configure input amplifier gain to cover a range of different voltage scales is highly flexible, allowing device optimization for multiple uses, including both mouse and rat, but also for other entirely non-neurological applications.

As future miniaturized technology solutions become available, the capabilities of such un-tethered systems can only become more sophisticated, and perhaps open a door to a new chapter in neuroscience discovery in the coming years.

REFERENCES

[1] Crouch, B., Sommerlade, L., Veselcic, P., Riedel, G., Schelter, B., Platt, B., 2018a. Detection of time-, frequency- and direction-resolved communication within brain networks. Sci. Rep. 8, 1825. https://doi.org/10.1038/s41598-018-19707-1

[2] Crouch, B., Yeap, J.M., Pais, B., Riedel, G., Platt, B., 2018b. Of mice and motion: Behavioural-EEG phenotyping of Alzheimers disease mouse models. J. Neurosci. Methods. https://doi.org/https://doi.org/10.1016/j.jneumeth.2018.06.028

[3] Kadam, S. D., D'Ambrosio, R., Duveau, V., Roucard, C., GarciaCairasco, N., Ikeda, A., ... and Kelly, K. M. (2017). Methodological standards and interpretation of videoelectroencephalography in adult control rodents. A TASK 1WG 1 report of the AES/ILAE Translational Task Force of the ILAE. Epilepsia, 58, 10-27.

[4] Chiesa, R., Restelli, E., Comerio, L., Del Gallo, F., and Imeri, L. (2016). Transgenic mice recapitulate the phenotypic heterogeneity of genetic prion diseases without developing prion infectivity: Role of intracellular PrP retention in neurotoxicity. Prion, 10(2), 93-102.

[5] Holth, J. K., Mahan, T. E., Robinson, G. O., Rocha, A., and Holtzman, D. M. (2017). Altered sleep and EEG power in the P301S Tau transgenic mouse model. Annals of clinical and translational neurology, 4(3), 180-190.

[6] Lampert, T., Plano, A., Austin, J., and Platt, B. (2015). On the identification of sleep stages in mouse electroencephalography time-series. Journal of neuroscience methods, 246, 52-64.

[7] Liu, Z., Wang, F., Tang, M., Zhao, Y., and Wang, X. (2019). Amyloid and tau are involved in sleep disorder in Alzheimer's disease by orexin A and adenosine A (1) receptor. International journal of molecular medicine, 43(1), 435-442.

[8] Yamazaki, K., Yamaguchi, M., Baranoski, L., Bard, J., Boyse, E. A., and Thomas, L. (1979). Recognition among mice. Evidence from the use of a Y-maze differentially scented by congenic mice of different major histocompatibility types. Journal of Experimental Medicine, 150(4), 755-760.

[9] Ma, M. X., Chen, Y. M., He, J., Zeng, T., and Wang, J. H. (2007). Effects of morphine and its withdrawal on Y-maze spatial recognition memory in mice. Neuroscience, 147(4), 1059-1065.

[10] Gerlai, R., Marks, A., and Roder, J. (1994). T-maze spontaneous alternation rate is decreased in S100! b transgenic mice. Behavioral neuroscience, 108(1), 100.

[11] Moreira, F. A., and Guimares, F. S. (2005). Cannabidiol inhibits the hyperlocomotion induced by psychotomimetic drugs in mice. European journal of pharmacology, 512(2-3), 199-205.

[12] Turri, M. G., Talbot, C. J., Radcliffe, R. A., Wehner, J. M., and Flint, J. (1999). High-resolution mapping of quantitative trait loci for emotionality in selected strains of mice. Mammalian Genome, 10(11), 1098-1101.

[13] Schwarzbold, M. L., Rial, D., De Bem, T., Machado, D. G., Cunha, M. P., dos Santos, A. A., and Rodrigues, A. L. S. (2010). Effects of traumatic brain injury of different severities on emotional, cognitive, and oxidative stress-related parameters in mice. Journal of neurotrauma, 27(10), 1883-1893.

[14] Arabo, A., Potier, C., Ollivier, G., Lorivel, T., and Roy, V. (2014). Temporal analysis of free exploration of an elevated plus-maze in mice. Journal of Experimental Psychology: Animal Learning and Cognition, 40(4), 457.

[15] https://www.panlab.com/en/products/smart-video-tracking-software-panlab

[16] Raghavan, A., Wilson, A., Wend, C., Alexander, A., Habela, C., and Nauen, D. (2018). Open-source system for millisecond-synchronized continuous video-EEG. Epilepsy research, 145, 27-30.

[17] Rensing, N., Moy, B., Friedman, J. L., Galindo, R., and Wong, M. (2018). Longitudinal analysis of developmental changes in electroencephalography patterns and sleep-wake states of the neonatal mouse. PloS one, 13(11), e0207031.

[18] Bin, N. R., Song, H., Wu, C., Lau, M., Sugita, S., Eubanks, J. H., and Zhang, L. (2017). Continuous monitoring via tethered electroencephalography of spontaneous recurrent seizures in mice. Frontiers in behavioral neuroscience, 11, 172.

[19] Zayachkivsky, A., Lehmkuhle, M. J., and Dudek, F. E. (2015). Long-term Continuous EEG Monitoring in Small Rodent Models of Human Disease Using the Epoch Wireless Transmitter System. Journal of visualized experiments : JoVE, (101), e52554. doi:10.3791/52554

[20] Lundt A, Wormuth C, Siwek ME, et al. EEG Radiotelemetry in Small Laboratory Rodents: A Powerful State-of-the Art Approach in Neuropsychiatric, Neurodegeneration, and Epilepsy Research. Neural Plast. 2015;2016:8213878. doi:10.1155/2016/8213878

[21] Jyoti, A., Plano, A., Riedel, G. and Platt, B. EEG, activity, and sleep architecture in a transgenic APPswe/PSEN1A246E Alzheimers disease mouse. J Alzheimers Dis 22(3), 873887 (2010).

[22] Latanov, V., Wolfer, D. P., Lipp, H. P., Vyssotski, A. L., Serkov, A. N., Itskov, P. M., and Dell'Omo, G. (2005). Miniature neurologgers for flying pigeons. physiology.

[23] Vyssotski, A. L., Serkov, A. N., Itskov, P. M., Dell'Omo, G., Latanov, A. V., Wolfer, D. P., and Lipp, H. P. (2006). Miniature neurologgers for flying pigeons: multichannel EEG and action and field potentials in combination with GPS recording. Journal of neurophysiology, 95(2), 1263-1273.

[24] Bailey, C., et al. A miniaturized 4-Channel, 2KSa/sec biosignal data recorder with 3-Axis accelerometer and infra-red timestamp function. In Seventh International Conference on Sensor Technologies and Applications, Barcelona, Spain, 2013.

[25] Bailey, C., Austin, J., Hollier, G., Moulds, A., Freeman, M., Fargus, A., and Lampert, T. (2015). Evaluating a Miniature Multisensor Biosignal Recorder for Unsupervised Parkinson's Disease Monitoring. Sensors and Transducers, 184(1), 66.

[26] Weiergrber, M., Papazoglou, A., Broich, K., and Mller, R. (2016). Sampling rate, signal bandwidth and related pitfalls in EEG analysis. Journal of neuroscience methods, 268, 53-55.

[27] Demanuele, C., James, C. J., and Sonuga-Barke, E. J. (2007). Distinguishing low frequency oscillations within the 1/f spectral behaviour of electromagnetic brain signals. Behavioral and Brain Functions, 3(1), 62.

[28] Gagnon-Turcotte, G., Maghsoudloo, E., Messaddeq, Y., De Koninck, Y., and Gosselin, B. (2017, June). A wireless photostimulator for optogenetics with live animals. In 2017 15th IEEE International New Circuits and Systems Conference (NEWCAS) (pp. 193-196). IEEE.

[29] Platt, B., Drever, B., Koss, D., Stoppelkamp, S., Jyoti, A., Plano, A., Riedel, G. (). Abnormal cognition, sleep, EEG and brain metabolism

in a novel knock-in Alzheimer mouse, PLB1. PloS one, 6(11), e27068. doi:10.1371/journal.pone.0027068

[30] Jyoti, A., Plano, A., Riedel, G., and Platt, B. (2015). Progressive age-related changes in sleep and EEG profiles in the PLB1Triple mouse model of Alzheimers disease. Neurobiology of aging, 36(10), 2768-2784.

[31] Vogler, E. C., Flynn, D. T., Busciglio, F., Bohannan, R. C., Tran, A., Mahavongtrakul, M., and Busciglio, J. A. (2017). Low Cost Electrode Assembly for EEG Recordings in Mice. Frontiers in neuroscience, 11, 629. doi:10.3389/fnins.2017.00629

[32] Tobler, I., Kopp, C., Deboer, T., and Rudolph, U. (2001). Diazepam-induced changes in sleep: role of the alpha 1 GABA(A) receptor subtype. Proceedings of the National Academy of Sciences of the United States of America, 98(11), 64646469. doi:10.1073/pnas.111055398

[33] Colgin, L.L., 2016. Rhythms of the hippocampal network. Nat. Rev. Neurosci. https://doi.org/10.1038/nrn.2016.21

[34] Chen, Z., Resnik, E., McFarland, J.M., Sakmann, B., Mehta, M.R., 2011. Speed controls the amplitude and timing of the Hippocampal Gamma rhythm. PLoS One 6. https://doi.org/10.1371/journal.pone.0021408

[35] Li, J.Y., Kuo, T.B.J., Hsieh, I.T., Yang, C.C.H., 2012. Changes in hippocampal theta rhythm and their correlations with speed during different phases of voluntary wheel running in rats. Neuroscience. https://doi.org/10.1016/j.neuroscience.2012.04.020

[36] Pluciska, K., Crouch, B., Yeap, J.M., Stoppelkamp, S., Riedel, G., Platt, B., 2018. Histological and Behavioral Phenotypes of a Novel Mutated APP Knock-In Mouse. J. Alzheimers Dis. 65, 165180. https://doi.org/10.3233/JAD-180336

[37] Koenig, T., Studer, D., Hubl, D., Melie, L., Strik, W.K., 2005. Brain connectivity at different time-scales measured with EEG. Philos. Trans. R. Soc. B Biol. Sci. https://doi.org/10.1098/rstb.2005.1649

[38] Sommerlade, L., Thiel, M., Mader, M., Mader, W., Timmer, J., Platt, B., Schelter, B., 2015. Assessing the strength of directed influences among neural signals: An approach to noisy data. J. Neurosci. Methods 239, 4764. https://doi.org/10.1016/j.jneumeth.2014.09.007

[39] OKeefe, J., Dostrovsky, J., 1971. The hippocampus as a spatial map. Preliminary evidence from unit activity in the freely-moving rat. Brain Res. https://doi.org/10.1016/0006-8993(71)90358-1

[40] Hafting, T., Fyhn, M., Molden, S., Moser, M.B., Moser, E.I., 2005. Microstructure of a spatial map in the entorhinal cortex. Nature. https://doi.org/10.1038/nature03721

[41] Lever, C., Burton, S., Jeewajee, A., OKeefe, J., Burgess, N., 2009. Boundary Vector Cells in the Subiculum of the Hippocampal Formation. J. Neurosci. https://doi.org/10.1523/JNEUROSCI.1319-09.2009

[42] Kropff, E., Carmichael, J.E., Moser, M.B., Moser, E.I., 2015. Speed cells in the medial entorhinal cortex. Nature 523, 419424. https://doi.org/10.1038/nature14622

[43] Mimica, B., Dunn, B.A., Tombaz, T., Bojja, V.P.T.N.C.S., Whitlock, J.R., 2018. Efficient cortical coding of 3D posture in freely behaving rats. bioRxiv. https://doi.org/10.1101/307785

[44] Fu, T.M., Hong, G., Zhou, T., Schuhmann, T.G., Viveros, R.D., Lieber, C.M., 2016. Stable long-term chronic brain mapping at the single-neuron level. Nat. Methods. https://doi.org/10.1038/nmeth.3969

Chris Bailey Dr. Chris Bailey, is a Senior Lecturer in Microelectronics and Computer Systems. He joined the Advanced Computer Architectures Group, at the University of York in 1999, exploring low power systems design, and he is currently a member of The Healthcare and Well-being research theme within the Department of Computer Science. He received a PhD in 1996, and most recently worked during industrial secondment on a 65nm CMOS ASIC Design and fabrication project.

Jim Austin Prof. Jim Austin, is Professor of Neural Computing and has interests in massively parallel array processing, scalability, pattern matching architectures, and data analytics. In 2012, Professor Austin Received The Times Higher Education Award for the Outstanding Research Team of the Year for work on distributed air-craft maintenance data-analytics. He is also CEO of Cybula Ltd, a successful UK technology research and development consultancy.

Bettina Platt Professor Bettina Platt holds the Chair of Translational Neuroscience at the University of Aberdeen. She is an expert in dementia research and heads a multi-disciplinary research team that investigates aspects of brain function and malfunction from the single molecule to the systems level. Her portfolio comprises national and international collaborations that have brought together novel research strategies and technologies to improve experimental dementia research, from bench to bedside.

Anthony Moulds Anthony Moulds is an experienced electronics engineer and holds the post of Senior Experimental Officer in the Department of Computer Science, University of York. He has significant experience in the development of ultra low-power systems and particular expertise in the design of intelligent miniaturized power-efficient hardware and devices.

Barry Crouch Dr Barry Crouch is a post-doctoral research fellow with the University of Aberdeen. He joined the translational neuroscience group in 2016 immediately after obtaining a PhD for his work on cellular pathology in schizophrenia. His present research is focused on translating recent improvements in electroencephalography (EEG) technology and analytics into clinical and pre-clinical research applications. His most recent work has centred around development of EEG based diagnosis tools for early detection of Alzheimers disease.